Proc. at 3rd National Conference
on Synchrotron Radiation Instrumentation
Brookhaven National Lab., Sept. 12-14, 1983.

BNL 33694

CONF-830910--3

BNL--33694

DE84 001461

APPLICATION OF SILICON CARBIDE TO SYNCHROTRON RADIATION MIRRORS*

P. Z. Takacs
Instrumentation Division
Brookhaven National Laboratory
Upton, New York 11973

T. L. Hursman and J. T. Williams
TRW Space and Technology Group
Applied Technology Division
Redondo Beach, California 90278

September 1983

* This research was supported in part by the U. S. Department of Energy: Contract No. DE-AC02-76CH00016.

DISCLAIMER

APPLICATION OF SILICON CARBIDE TO SYNCHROTRON-RADIATION MIRRORS*

P. Z. Takacs
Instrumentation Division
Brookhaven National Laboratory
Upton, New York 11973

T. L. Hursman and J. T. Williams
TRW Space and Technology Group
Applied Technology Division
Redondo Beach, California 90278

Abstract

Damage to conventional mirror materials exposed to the harsh synchrotron radiation (SR) environment has prompted the SR user community to search for more suitable materials. Next-generation insertion devices, with their attendant flux increases, will make the problem of mirror design even more difficult. A parallel effort in searching for better materials has been underway within the laser community for several years. The technology for dealing with high thermal loads is highly developed among laser manufacturers. Performance requirements for laser heat exchangers are remarkably similar to SR mirror requirements. We report on the application of laser heat exchanger technology to the solution of typical SR mirror design problems. The superior performance of silicon carbide for laser applications is illustrated by various material trades studies, and its superior performance for SR applications is illustrated by means of model calculations.

* This research was supported in part by the U. S. Department of Energy: Contract No. DE-AC02-76CH00016.

Scope

TRW has been in the business of laser system and component development for 14 years. Contributing to the success of the TRW programs has been the development of mirror heat exchangers and the engineering expertise to design systems that will withstand the harsh laser environment. Performance requirements of optical elements for use in synchrotron radiation (SR) beam lines are very similar to those of TRW optics. It is our intention to apply the heat exchanger engineering and fabrication technology that has been developed at TRW to SR mirror engineering and fabrication problems. The present discussion focuses attention to the fact that SiC has emerged as the material of choice for both SR and laser applications, and that the technology that has been developed by the laser community exists to provide mirror heat exchangers for both user communities.

Statement of the Problem

The search for a better SR mirror material was prompted by degradation and failure of commonly-used optical materials upon exposure to intense x-ray fluxes and heat loads from synchrotron storage rings. Experiments at SPEAR in 1973-74 resulted in surface and substrate damage to quartz mirrors coated with Pt, Au and Ni films[1,2]. ZERODUR mirrors at DESY suffered from severe surface crazing[2]. The quartz mirrors at SPEAR were replced with cooled pt-coated Cu mirrors, whose surfaces gradually degraded with an attendant increase in surface roughness from 64 Å RMS to 186 Å RMS[3]. Proper handling of Cu is a severe problem during fabrication and use. Superpolished fused silica mirrors were shown by NPL researchers to suffer from several degrading effects after exposure to the beam from the DESY synchrotron[4,5]. Gross figure changes were observed, which were attributed to a structural volume

contraction effect caused by approach of the glassy material toward thermodynamic equilibrium following the breaking of weak molecular bonds by ionizing radiation and/or heat. Surface topography in these mirrors was also observed to degrade upon exposure to the DESY beam. A systematic investigation of candidate mirror materials under worst-case uncoooled irradiation conditions at DORIS was performed by Zietz, Saile and Haelbich[6]. X-ray fluxes ranged from 29 W/cm^2 to 84 W/cm^2 on the samples. Only the chemical vapor deposited (CVD) SiC sample survived with no apparent surface structure or figure change. Our own experience at the NSLS indicates significant degradation of the surface of normal incidence Cu mirrors coated with Al and MgF_2 when exposed to peak power densities from the VUV ring on the order of 5 W/cm^2 over a period of one year.

Causes for SR mirror degradation and failure noted above can be divided into two classes: synchrotron radiation-related causes, and intrinsic materials and engineering design problems. The SR-related causes include damage from x-ray radiation, high thermal loads, which cause local surface heating and bulk temperature rise effects, and photochemical carbon deposition. The material and enginering problems include microcreep and stress relaxation, inadequate mount design, inadequate cooling system design, coating adhesion problems, susceptibility to corrosion, and accidental handling errors. In most cases the beamline designer has no control over the SR parameters causing the mirror problems. He only has control over the material properties of the components receiving the SR flux. Proper design of a mirror and its mounting system, including cooling system, becomes a complex engineering problem, for which no easy solutions exist. In general, each initial element in a beamline presents a unique design problem, owing to the diverse requirements of the downstream experiments.

The trend in future SR beamline parameters is indicated in Table I for present and proposed beamline construction at the NSLS. The second column shows the trend toward higher brightness insertion device sources - wigglers and undulators - that have more total power packed into a more highly collimated radiation cone than is true for a conventional arc source. Column four shows the range of normal incidence beam power densities on components placed at various distances away from the source where they will most likely be used. The last two columns show power densities for typical first-mirror configurations. In most cases the extreme grazing angle and high reflectivity lowers the absorbed power density to reasonable levels. But for some applications, where beam extraction is desired with a grazing angle that exceeds the critical angle for total reflection, power densities will rapidly increase to troublesome levels.

SR Mirror Requirements

Some generalizations can be made about requirements for SR mirrors, especially the first reflector in a SR beamline, which is usually subjected to the most intense and hardest x-ray flux, and any other mirror upon which a focussed source image falls. Most glass, glass-ceramic, and metal materials fail to meet one or more of the following requirements: They must operate in ultra high vacuum (UHV) at pressures less than 10^{-9} Torr and must not be a source of vacuum contamination. They must resist damage from intense x-ray irradiation. They must stabilize rapidly (1 minute) upon initial exposure to high flux loading, and they must maintain surface figure under thermal loading. High thermal loads require active cooling capability. They must be polishable to a super-smooth low-scatter surface finish, on the order of 5 Å RMS roughness or less, and maintain that surface finish and quality. They must be chemically inert, and easily cleaned and recoated in the event of a

vacuum accident or as a result of long term exposure to low-level contamination. And they must be available in long, narrow shapes with aspheric surface figures at a reasonable cost for the finished product.

Laser Mirror Heat Exchanger Requirements

Mirrors for laser applications are subject to requirements similar to SR mirrors. The mirrors for laser systems must operate in a vacuum (5 to 20 Torr), be chemically inert, stabilize rapidly (1 second) upon initial exposure to high flux loading, maintain surface figure while under laser flux loading, have and maintain low-scatter surfaces, be figured with a surface figure error of less than $\lambda/10$ PV, be polishable to a surface finish of less than 40 Å RMS, and operate under absorbed laser flux intensities of greater than 300 watts/cm^2. Specific requirements for both laser and SR mirrors can vary considerably depending upon the operational scenario. Laser and SR mirror cooling requirements depend upon the incident flux, angle of incidence, and the optical coating.

The requirements definition process is critical to establishing a good foundation for design and analysis of SR mirror heat exchangers. TRW has extensive experience in developing design criteria to meet the system operational scenario and requirements. Accurate and orderly rquirements must be established to develop an optimum mirror heat exchanger design for best performance, ease of fabrication, and at minimum cost. Table II shows a list of typical requirements for mirror heat exchanger design. Additionally, all critical interfaces with other systems and subsystems, both physical and functional, are defined in this process.

TRW has developed efficient water-cooled and ammonia-cooled heat exchangers for various laser programs in the form of mirrors, scrapers, clippers, dumps, and calorimeters, and has used several types of thermal-skin

heat exchanger designs in these laser systems. Mirrors, clippers, and dumps have used pin-fin, pin-post, diamond-fin, straight channel, and heat pipe designs. The thermal skin-type heat exchangers are built by brazing or diffusion bonding together machined or etched plates, then figuring, polishing, and optically coating the surfaces. TRW has extensive experience using various materials in heat exchangers such as molybdenum, beryllium, Be-Cu, tungsten, tungsten carbide, silicon carbide, and graphite-Al and graphite-Mg composites. The physical and mechanical properties of some of these materials are listed in Table III. We have successfully demonstrated some of these various heat exchanger designs in numerous high-flux absorbing applications without a single failure. In addition, TRW has extensive experience in utilizing a broad range of materials for uncooled mirrors: metals, carbides, oxides, nitrides, cermetals, glasses, glass-ceramics and composites. The uncooled mirrors have been fabricated from ULE, Zerodur, OFHC copper, Be-Cu copper, SiO_2, SiC, and aluminum.The absorbed flux for these systems varies as a function of the maximum allowable distortion for each type of laser resonator configuration. Each resonator configuration has various levels of sensitivity and insensitivity relative to specific mirror distortions. Based on our experience with laser optical components, an extremely important consideration in the design of mirror systems is the mounting hardware. Mirrors that are subjected to severe thermal loading require carefully engineered mounts and holding fixtures. TRW has the capability and expertise to design appropriate mounting hardware to suit each individual installation.

Mirror Heat Exchanger Distortions

As indicated in Table I, future SR beam line fluxes will be increasing to levels at which SR mirrors will need to be actively cooled to prevent

thermal deformation and distortion of the mirror surface. An example of a heat exchanger with three-pass (three-level) cooling designed for laser applications is shown in Figure 1. The design features a thin faceplate with cooling channels immediately below the surface. This design allows the heat to be removed in close proximity to the point at which it is applied and isolates the substrate and mount from the heat load. A typical non-uniform laser mirror irradiance profile is shown in Figure 2 with the predicted thermal surface distortion response. Flowing coolant introduces additional distortion effects into the mirror system: coolant jitter, pressure ripple, pressure tilt and astigmatism. Figure 3 illustrates the effect of pressure ripple above the coolant cavity channel that is filled with high pressure fluid. An overall surface tilt between the inlet and outlet sides results from the difference in the pressure ripple effect between the high pressure inlet side and low pressure outlet side. Thermal growth of the faceplate is greatest over the land area between the coolant channels and tends to cancel the effects of the pressure ripple.

Thermal and pressure distortions of laser mirrors have been studied extensively at TRW because they generally have the greatest impact on mirror distortions and resulting degradation to the beam. TRW has developed a number of analysis codes that can be incorporated as units of the thermal and structural deformation analysis modules for evaluating SR mirror distortions. The analysis of distortions is divided into two parts; (1) local distortions of the heat exchanger, and (2) overall distortions of the mirror and substrate. The local and overall mirror distortion analyses are combined to calculate the total mirror face distortion. TRW has developed a 3-D semi-automatic interactive first-order computer analysis program for assessing mirror distortions. This computer program is used to bound the problem and

develop mirror heat exchanger concepts. For detailed analysis of mirror heat exchangers, finite element modelling is performed. TRW uses NASTRAN models for both the thermal and structural deformation analysis of mirror heat exchangers.

Search for a Better Laser and SR Mirror Material

TRW has conducted several mirror heat exchanger material performance assessments over the past several years to identify a mirror heat exchanger material that offers better performance than molybdenum and copper, which are the current standards. Some were based on figure-of-merit assessments and some on finite thermal and structural element modelling and analyses. Materials examined included silicon, graphite/carbon (c/c), carbides and metal matrix composites. These alternative materials provide the following potential advantages over molybdenum and copper:

1. Performance Improvement
   - Improved beam quality or lower mirror surface distortion.
   - Increased power absorption capability.
   - Reduced coolant requirements.
2. Temporal Stability
   - Brazeless technology in the heat exchanger.
   - Improved microcreep material properties.
3. Producibility
   - Eliminates braze joint at the coolant passages.
   - Reduces cost.
   - Reduces procurement leadtime.
4. Flightweight
   - Reduction of 3 to 4 times the weight of molybdenum or copper.

Thermal and structural finite element models were utilized to predict the performance of a typical turning flat heat exchanger under a high power irradiation. The peak-to-average power ratio incident to the mirror heat exchanger used in this analysis was 3 to 1. Figure 4 shows the results of this analysis and a list of the materials evaluated. In this study the thickness of the heat exchanger substrates was varied to give constant weight. This figure illustrates the relative magnitude of the thermal distortions due to the linear thermal growth through the heat exchanger (irradiance mapping) and total distortion including bending (focus) for constant weight heat exchangers. It illustrates the strong influence substrate depth has on focus distortion. Other material parameters studied include maximum allowable heat load and distortion improvement, weight reduction and flux handling capability under constant geometry and constant coolant flow conditions. Performance results for constant geometry and constant flow studies are shown in Figure 5 for materials that exceed the performance of the molybdenum baseline material and offer improved beam quality, future potential to handle higher absorbed heat loads, and reduction in coolant requirements. Enhancement of optical stability is feasible with these materials in that they offer brazeless bonding technologies in the heat exchanger area and also may exhibit extremely good mirror-creep properties.

To provide a correlation of all the analyses, a conceptual design of a three-pass mirror heat exchanger turning flat was generated as shown in Figure 6. The mirror heat exchangers for all the materials and conditions were subjected to the same beam load conditions. The analysis was parametric so that distortion, weight and coolant flowrate comparisons could be made relative to the baseline molybdenum design. The comparisons illustrated in Figure 6 show that silicon carbide is a strong performer for distortion with

constant geometry and flow. Silicon carbide yields a 60 per cent improvement in distortion compared to molybdenum or tungsten carbide on silicon carbide. Weight is compared with both constant geometry and constant distortion and flow parameters. For constant geometry, both silicon carbide and tungsten carbide on silicon carbide offer significant weight reductions. For a weight comparison with constant distortion and flow, analysis shows that silicon carbide can offer 4.2 times the weight reduction compared to molybdenum. Comparing flow rate for constant distortion and geometry, the silicon carbide system offers a 40 per cent reduction in flow rate compared to molybdenum. Results of the finite element and parametric analyses indicate that both tungsten carbide heat exchangers on a silicon carbide substrate and an all silicon carbide heat exchanger assembly are excellent near-term replacement materials systems for molybdenum in laser systems.

In recent years, considerable attention has also been focused toward the development of alternative materials for SR applications that overcome the limitations of metal and glass optics. One of the most promising candidates to emerge as an SR heat exchanger substrate is silicon carbide (SiC) ceramic material. The sintered and reaction bonded materials, and also chemical vapor deposited (CVD) SiC, have been the subject of several recent investigations to determine its suitability for SR applications[2,6-14]. Results of these studies have been extremely encouraging. The advantages of SiC over current SR mirror materials are many:

- Hardness - resists damage, easily polishable.
- Capable of being super-polished to less than 5 Å RMS roughness level.
- Low thermal expansion coefficient and high thermal conductivity - maintains surface figure under thermal loading.
- Rapid thermal stabilization time.

- Excellent radiation damage resistance.
- Ultrahigh vacuum compatible.
- Capable of being operated at elevated temperatures with no degradation in performance.
- Chemically inert - can be cleaned and recoated without damage to the surface finish or to any surface features, such as ion-milled diffraction gratings.

TRW Silcon Carbide Mirror Heat Exchanger Design and Fabrication Experience

A mirror heat exchanger assembly consists of 1) a substrate for support of the thermal skin portion of the assembly and distribution of the coolant, 2) a faceplate, 3) midplates, 4) a backplate, and 5) a mounting ring. Laser mirror heat exchangers can be round, square, and rectangular in shape. They can be configured as planos, spheres, aspheres, toroids, cylinders, and conics. They can range in size from a few centimeters to several meters in length or diameter. The heat exchanger thickness can vary from 5 centimeters to 15 centimeters. Figure 7 is a photograph of a typical three-pass (three-level) heat exchanger subassembly showing these details. Figure 8 shows a heat exchanger assembly in its mount ring prior to figuring, polishing, and optical coating. Figures 9 and 10 show isometric cross-sections of typical laser turning flat and scraper mirror heat exchangers, respectively. Based on the material trades studies discussed earlier, TRW has recently been developing silicon carbide laser mirror heat exchangers. The design, fabrication, acceptance testing, figuring, polishing, and optical coating of silicon carbide mirror heat exchangers has been accomplished. Figure 11 shows a silicon carbide substrate and steel mount ring prior to assembly by brazing. Figure 12 shows the green and fully sintered alpha-type silicon carbide mirror heat exchanger assembly details. The sintered details have undergone an

18 per cent shrinkage from the green to the dense state as is easily seen in Figure 12. These details were then diffusion bonded together to complete the single-pass heat exchanger. Two of the faceplate and substrate assemblies were diffusion bonded at 2000°C to form a brazeless monolithic heat exchanger. Figure 13 shows one of the single-pass silicon carbide heat exchangers directly after diffusion-bonding. The heat exchangers were then acceptance tested and figure polished. Three acceptance test methods were used to evaluate the heat exchanger integrity. A 50-psi helium leak test was successfully conducted on the heat exchangers. No leaks were found at a vacuum level of 10^{-6} Torr. A flow versus ΔP curve was also generated. The flow data at different ΔP values was within 10 per cent of the calculated values. The final acceptance test, hydrostatic pressure/leak, was conducted on these heat exchangers. The hydrostatic pressure was 1.5 times the inlet pressure of 500 psi. The heat exchanger survived the 750-psi burst proof pressure and was found leak-free. One of the two diffusion-bonded heat exchangers was cut into two halves, and the cut surface was ground and polished. At the diffusion bond joint a chemical etch and a photomicrograph were made to verify that the diffusion bond was complete and void free. Figure 14 shows this sectioned heat exchanger and Figure 15 the 200X photomicrograph at the diffusion bond joint. No voids can be found and the bond joint is complete.

TRW has developed the figuring and polishing capabilities of several SiC materials: sintered alpha-SiC; KXOX, which is a two-phase reaction bonded material containing free silicon; and CVD SiC deposited on a sintered alpha substrate. A single-pass, diffusion-bonded, sintered alpha heat exchanger was figured as a plano and polished. As the sintered alpha material is approximately 98 per cent dense, at best a finish of 50 Å RMS was achieved.

The second silicon carbide material, KXOX, is a two-phase material: ten per cent of the composition is silicon and the remainder is alpha-silicon carbide. The resultant structure is 100 per cent dense, which allows better surface finishes to be obtained. More than thirty 3.8 cm diameter test specimens were polished with surface roughness values between 4 and 20 Å RMS as measured by optical and stylus profilometry. Over 80 per cent of the samples had roughness values below 12 Å RMS. A CVD SiC coating was applied to a sintered alpha substrate. The coating was 0.65 mm thick. It was then superpolished to a 5 Å RMS surface roughness. Several of both of the KXOX and CVD coated silicon carbide substrates were successfully coated with multilayer dielectrics. The optical reflectivity averaged above 99.9 per cent for all the test samples at the design wavelengths.

The only differences foreseen between the laser and SR mirror heat exchanger designs are the shape of the mirror, the method used to provide the coolant into the mirror while in ultra high vacuum (10^{-9} Torr), and a relaxation of the stringent figure distortion requirements for laser mirrors. The long narrow rectangular shapes of SR x-ray mirrors and the cylindrical surface figures can be fabricated using the same materials and processes utilized to produce the laser mirror heat exchangers. The design, analysis, and manufacturing technologies are in hand to produce the SR mirrors. The coolant porting must be accomplished such that the joints between the heat exchanger and the coolant lines are made outside the SR vacuum chamber. This requirement has been previously met on actively cooled power dumps in nuclear fusion vacuum chambers using a similar heat exchanger porting design approach.

TRW Case Studies on Proposed NSLS SR Mirrors

A study was performed to characterize and obtain relative performance

data for SR copper mirrors and silicon carbide mirrors. The study was conducted for two cases:

1. Uncooled wiggler copper mirror at 2° grazing angle.
2. Cooled wiggler mirror heat exchanger at a 12° grazing angle.
3. Cooled wiggler mirror heat exchanger at a 1° grazing angle.

The methods used to conduct the analysis for these two cases are:

1. Discrete numerical methods for the uncooled wiggler mirror based upon the work in Reference 16.
2. For the cooled heat exchanger analysis, a computer program called Interactive Thermal Structural Optics Analysis Program (ITSAP) was used. This allows the user to interactively input various geometric, materials and operating criteria, properties and constraints in order to obtain heat exchanger performance data.

The performance criteria in this study was based solely upon thermal and mechanical considerations. However, other important criteria which may ultimately limit the choice of a material or design are:

1. Coatings and coating survivability.
2. Substrate polishability.
3. Substrate degradation due to radiation exposure and environment.
4. Surface finish degradation of the mirror substrate.
5. Coating vs. substrate compatibility.
6. Maintainability.

It is very important to point out that in making optimal selections of candidate mirror types and materials that all of these issues and factors must be evaluated, and in no sense did this analysis attempt to fold in all of these factors. What was accomplished was to point out and to identify very

important issues, and to provide performance data to be used in a more exhaustive engineering study for making SR mirror selections and designs.

Uncooled Wiggler Mirror

A discrete nodal thermal analysis was performed on an uncooled copper mirror located 10 meters from the source point in the Superconducting Wiggler beamline. The assumptions used in this analysis are:

1. 2° grazing angle of incidence.
2. 100 w/cm^2 incident power density.
3. Uniform distribution of incident flux.
4. 100% absorption of incident flux.
5. One dimensional model.
6. No losses from conduction, convection or radiation.

Figure 16 is a representation of the model that was analyzed. The temperatures were evaluated at the nodal points. A superposition of the assumed uniform distribution versus the gaussian or normal distribution of heat flux is included for comparison, both of which integrate to the same power. Figure 17 is the time response of the mirror; the temperature at three nodal points is indicated as a function of time in order to illustrate the steady rise in temperature throughout the mirror. One can see that, in the long term, some mechanism, e.g. cooling via heat exchanger technology, is needed to stabilize the system; otherwise steady state conditions will occur only after long times through radiative equilibrium, and in most cases will result in unacceptable high surface temperatures. Figure 18 illustrates thermal profiles through the depth of the mirror at several time intervals. It illustrates quite dramatically that the front surface region exprierces a tremendous temperature rise, while the back side exhibits only a very slow minimal response. This indicates that heat exchanger cooling would be most

effective near the front surface because back side cooling would provide little control of the front surface temperatures, offering only some overall thermal stability control.

Cooled Wiggler Heat Exchanger Mirror

Based on the uncooled mirror studies presented above, analyses were performed to develop first order performance characteristics of heat exchanger mirrors fabricated from Cu and SiC for two grazing incidence angles: 1° and 12°. The heat exchanger design is based upon the standard laser heat exchanger concept illustrated in Figure 1, but using only one level of heat exchanger channels. Two incident flux distributions are used in each calculation: a uniform rectangle distribution and a normal Gaussian distribution to more closely represent the actual flux profile. Faceplate thickness is 0.51 mm over the cooling channels; cooling channel width is 1.65 mm and web width is 0.38 mm for the present calculations. Results of the calculations are presented in Table IV for the 12° case and Table V for the 1° case. One can see that SiC outperforms Cu in each case by about a factor of four in terms of total RMS surface distortion from thermal and pressure effects. The worst case RMS slope errors calculated from the Gaussian peak distortion data, assuming a surface period of 2.03 mm, are 142 arc sec for Cu and 40 arc sec for SiC at the 12° angle, and 20.4 arc sec and 5.3 arc sec respectively at the 1° angle. The target design criteria is 10 arc sec. Only the SiC material meets the design criteria at the 1° angle; both materials exceed the 10 arc sec criteria at the 12° angle. Design parameters for SiC material would require minor revisions to meet the performance requirements, but significant changes would be required in the Cu HEX design. Orientation of the subsurface cooling channel direction relative to the plane of incidence and/or to the direction of dispersion in downstream beamline instruments has a bearing

on the design impact of slope errors from these types of heat exchangers. Slope errors along the direction of the cooling channels are of lesser magnitude than the illustrated values orthogonal to the channels. Note that for an increase in the mechanical performance afforded by SiC, a slight increase in surface temperature must be tolerated. The significantly higher modulus of elasticity of SiC over that of Cu (see Table III) and the lower coefficient of thermal expansion of SiC work in concert to produce a mechanically more stable heat exchanger. The advantages of silicon carbide as a heat exchange material based upon concepts now employed in laser technology applications offer a very significant potential in resolving related SR mirror problems.

REFERENCES

[1] J. L. Stanford, V.Rehn, D. S. Kyser, V. O. Jones, and A. Klugman, in Vacuum Ultraviolet Radiation Physics, (E. Koch, E. Haensel and C. Kunz, eds., Pergamon-Vieweg, Braunschweig, Germany, 1974). p. 783.

[2] V. Rehn and V. O. Jones, Opt. Eng. 17 (1978) 504.

[3] R. Z. Bachrach, S. A. Flodstrom and R. S. Bauer, Nucl. Instr. and Meth. 152 (1978) p. 135.

[4] A. Franks, K. Lindsey, P. R. Stuart and R. Morrell, in Workshop on X-Ray Instrumentation for Synchrotron Radiation Research, (H. Winick and G. Brown, eds., 1978), SSRL Report No. 78/04.

[5] A. Franks and M. Stedman, Nucl. Instr. and Meth. 172 (1980) 249.

[6] R. Zietz, V. Saile and R.-P. Haelbich, Proc. VI Int. Conf. on Vacuum Ultraviolet Radiation Physics, Charlottesville, Virginia (1980), III-42.

[7] W. J. Choyke, R. F. Farich and R. A. Hoffman, Appl. Optics 15 (1976) 2006.

[8] V. Rehn and W. J. Choyke, Nucl. Instr. and Meth. 177 (1980) 173.

[9] P. Z. Takacs, Topical Meeting on Non-Oxide Ceramics, South Yarmouth, Mass., sponsored by American Ceramic Society (Oct. 1981), BNL No. 30341.

[10] P. Z. Takacs, Nucl. Instr. and Meth. 195 (1982) 259.

[11] R. E. Engdahl, Proc. SPIE 315 (1981) 123.

[12] R. L. Gentilman and E. A. Maguire, Proc. SPIE 315 (1981) 131.

[13] M. M. Kelly and J. B. West, Proc. SPIE 315 (1981) 135.

[14] K. Lindsey, R. Morrell and M. J. Hanney, Proc. SPIE 315 (1981) 140.

[15] G. K. Green, Beam Power in Synchrotron Radiation. BNL No. 23745.

[16] S. V. Patankar, Numerical Heat Transfer and Fluid Flow, Hemisphere Publ. Corp./McGraw-Hill, New York (1980).

Table I. Present and Proposed NSLS Beamline Parameters

Device	Beam Size for Max Power Deposition*	Total Power	Beam Power Density*	Power Distribution Incident on Mirror*	Usage
VUV Arc	up to 90 mradθ 1.36 mradΨ	2.33 W/mradθ	19 W/cm^2 @ 3m 398 W/cm^2 @ 0.656m	19 W/cm^2 281 W/cm^2	$\alpha = 90^\circ$, U9A $\alpha = 45^\circ$, IR Beam Line
X-ray Arc	up to 50 mradθ 0.41 mradΨ	40 W/mradθ	400 W/cm^2 @ 5m	1.2 W/cm^2 4.0 W/cm^2	α = 3 mrad α = 10 mrad
SUW superconducting wiggler	39.6 mradθ (12 mradθ usable) 0.41 mradΨ	33.4 kW total 14.6 kW usable	1.51 kW/cm^2 @ 14m	4.5 W/cm^2	α = 3 mrad
HW Permanent Magnet Hybrid Wiggler	3 mradθ 0.41 mradΨ	3.5 kW	1.45 kW/cm^2 @ 14m	4.35 W/cm^2	α = 3 mrad, expect 99% power absorbed into multilayer coating
SXU Soft X-ray Undulator	0.25 mradθ 0.057 mradΨ	152W	5.4 kW/cm^2 @ 14m	54 W/cm^2	α = 10 mrad
FEL Undulator	0.131 mradθ 0.096 mradΨ	12W	954 W/cm^2 @ 10m	954 W/cm^2 9.54 W/cm^2	$\alpha = 90^\circ$ α = 10 mrad

*Vertical angle, Ψ, and power density determined by rectangle approximation. See BNL 23745 by G. K. Green.[15]

Table II. Typical Laser HEX Requirements

- DESIGN REQUIREMENTS
  - HEAT EXCHANGER ENVELOPE DIMENSIONS
  - HEAT EXCHANGER MATERIAL
  - HEAT EXCHANGER ENVIRONMENT
    - OPERATIONAL
    - NON-OPERATIONAL
  - HEAT EXCHANGER INTERFACES
    - MOUNT
    - COOLANT PORTS
  - COOLANT CHARACTERISTICS
  - HEAT EXCHANGER COOLED AREA
- THERMAL LOADING
  - THERMAL DESIGN PARAMETERS
  - ABSORBED POWER AREA (BEAM FOOTPRINT)
  - INCIDENT BEAM PROFILES
  - PERFORMANCE REQUIREMENTS/BEAM QUALITY
    - THERMAL DISTORTION
    - PRESSURE DISTORTION
    - JITTER RESPONSE
  - ABSORPTIVITY
- HEAT EXCHANGER FACEPLATE REQUIREMENTS
  - AS DELIVERED (READY FOR POLISH) FINISH
  - HOT WALL REQUIREMENTS
- GENERAL REQUIREMENTS
  - WEIGHT
  - FLOWRATE
  - LOADS
  - COOLANT
  - MATERIAL
  - ENVIRONMENTS
- MECHANICAL
  - ENVELOPE
  - MECHANICAL INTERFACES

Table III. Properties of Heat Exchanger Materials

	Material Mechanical Properties		Material Physical Properties							
	Modulus of Elasticity		Thermal Expansion Coefficient		Thermal Conductivity		Mass Density		Thermal Diffusivity	
	E		α		K		ρ		a	
	lb/in.^{2}	n/cm^2	in./in./°F	cm/cm/°C	Btu/ hr/°F ft	cal/cm sec °C	lb/in.^{3}	gm/cc	ft^2/hr	cm^2/se
Material	10^{-6}	10^6	10^{-6}	10^{-6}	-----	-----	-----	-----	-----	-----
Molybdenum	46.8	32.3	2.7	4.86	84.5	.3495	.369	10.24	2.05	0.53
Tungsten Carbide	93.9	64.8	2.5	4.54	70.0	.2895	.549	15.22	1.84	0.476
Tungsten	57.4	39.6	2.5	4.5	96.6	.3996	.699	19.38	2.36	0.61
Silicon Carbide	58.9	40.6	1.48	2.664	72.6	.3003	.113	3.14	1.19	0.309
Silicon	17.9	12.4	1.4	2.5	86.7	.3586	.083	2.31	3.76	0.97
Zerodur	13.1	9.06	5.0	9	0.94	.0039	.079	2.21	.031	0.008
ULE	9.79	6.75	1.67	3	0.774	.0032	.079	2.2	.0299	.0077
Copper	16.9	11.7	9.8	17.64	224	.9265	.322	8.94	4.3	1.12
Fused Silica	10.6	7.309	3.11	.56	.7959	.0033	.079	2.202	.0326	.0084

Table IV - HEX Performance Comparison for 12° Grazing Incidence

Single-pass design; Inlet coolant temperature 70°F;
Inlet coolant pressure 300 PSI; Coolant velocity 90 ft/sec

	COPPER		SILICON CARBIDE	
	I_{avg} = 625 W/cm^2	I_{peak} = 820 W/cm^2	I_{avg} = 625 W/cm^2	I_{peak} = 820 W/cm^2
THERMAL DEFLECTION OVER CHANNEL (μM)	.1297	.1698	.0598	.0783
PRESSURE DEFLECTION OVER CHANNEL (μM)	.0244	.0244	.0078	.0078
THERMAL DEFLECTION OVER WEB (μM)	.3647	.4579	.0793	.0996
RMS DISTORTION (μM)	.1834	.2305	.0519	.0652
SUBSTRATE BENDING IF HAD ONE CHANNEL (μM)	——	——	——	——
SURFACE TEMP. (°F) OVER CHANNEL	161.1	183.2	191.7	233.3
SURFACE TEMP. (°F) OVER WEB	156.0	176.2	165.7	188.6
INNER CHANNEL WALL TEMP. (°F)	146.4	164.0	146.4	164.0
END OF WEB TEMP. (°F)	119.7	130.7	113.0	122.4
PRESSURE DROP (PSI)	120.65	119.42	120.65	119.42
FILM COEFFICIENT (BTU/hr-ft^2-°F)	34411	36636	34411	36636

Table V - HEX Performance Comparison for 1° Grazing Incidence

Single-pass design; Inlet coolant temperature 70°F;
Inlet coolant pressure 300 PSI; Coolant velocity 45 ft/sec

	COPPER	SILICON CARBIDE		
	I_{avg} = 51.8 W/cm^2	I_{avg} = 51.8 W/cm^2		
THERMAL DEFLECTION OVER CHANNEL (μM)	.0113	.0052		
PRESSURE DEFLECTION OVER CHANNEL (μM)	.0261	.0069		
THERMAL DEFLECTION OVER WEB (μM)	.0559	.01181		
RMS DISTORTION (μM)	.033	.0085		
SUBSTRATE BENDING IF HAD ONE CHANNEL (μM)	———	———		
SURFACE TEMP. (°F) OVER CHANNEL	86.1	88.7		
SURFACE TEMP. (°F) OVER WEB	85.9	87.1		
INNER CHANNEL WALL TEMP. (°F)	84.8	87.1		
END OF WEB TEMP. (°F)	80.4	79.2		
PRESSURE DROP (PSI)	151.2	151.2		
FILM COEFFICIENT (BTU/hr-ft^2-°F)	15694	15694		

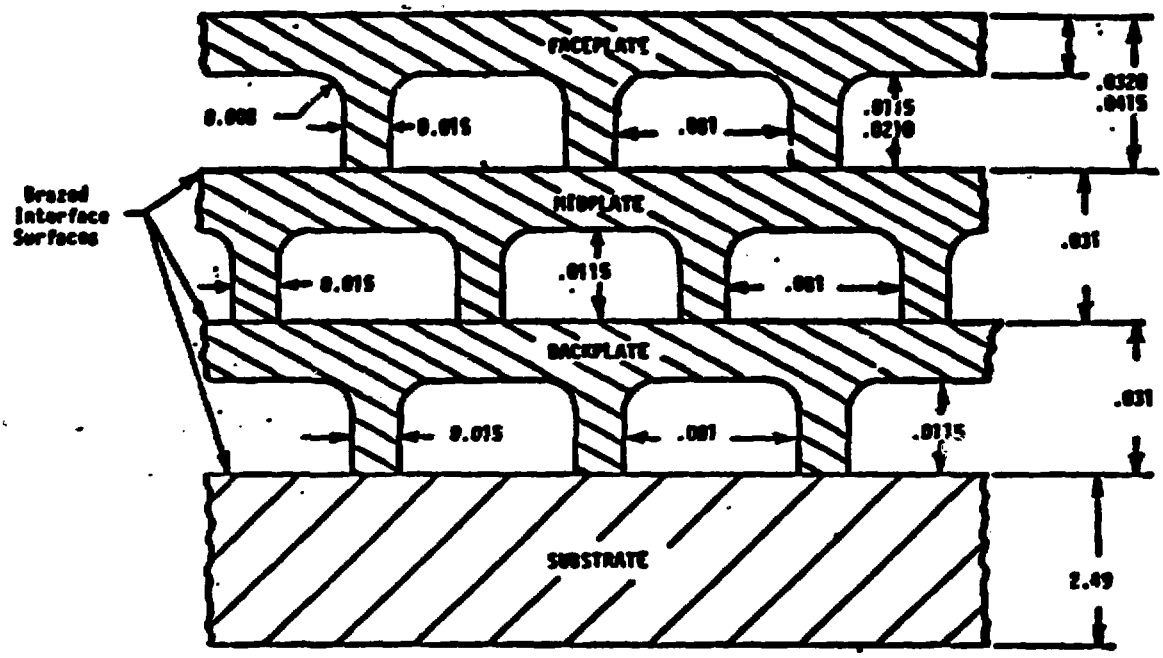

Figure 1. Cross-section of a typical laser mirror heat exchanger with three-pass (three-level) cooling.

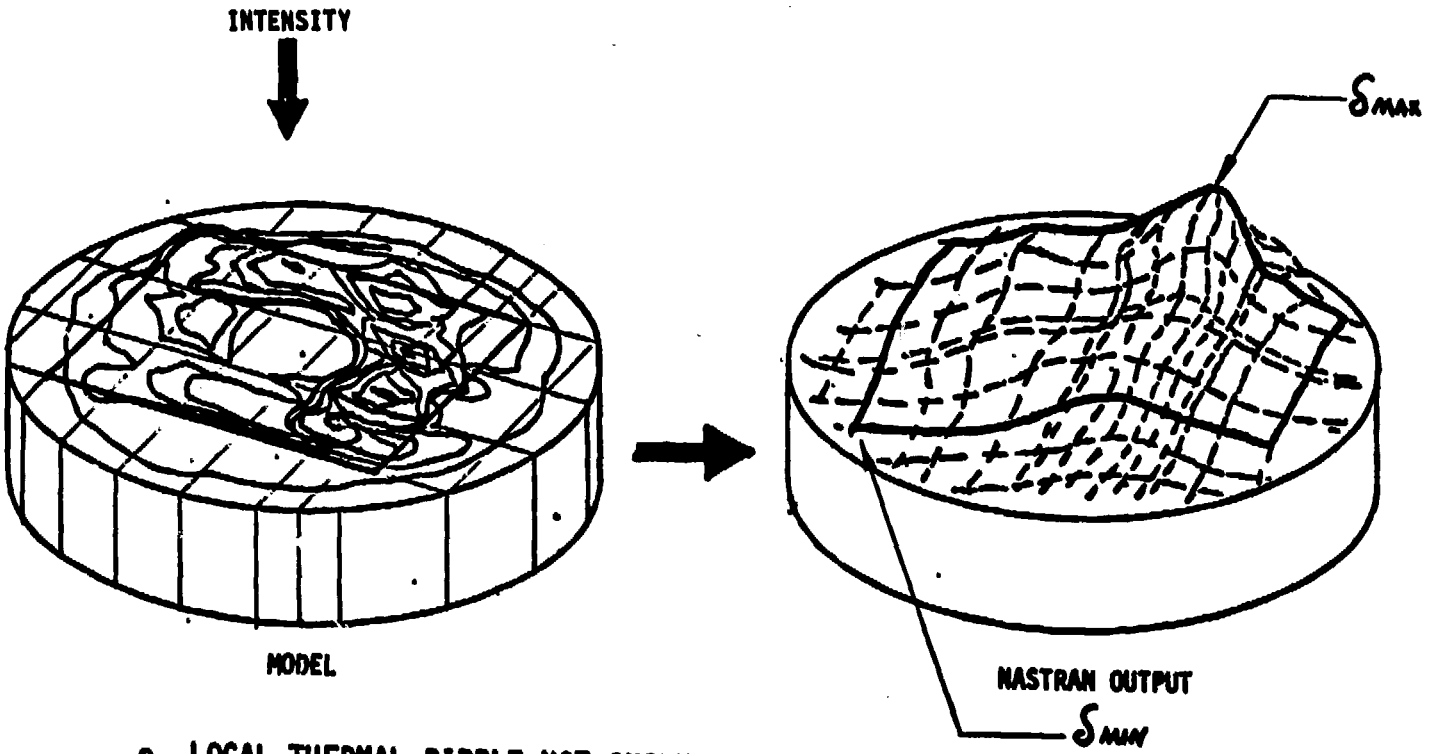

o LOCAL THERMAL RIPPLE NOT INCLUDED

Figure 2. Classical Example of Irradiance Mapping Surface Deflections

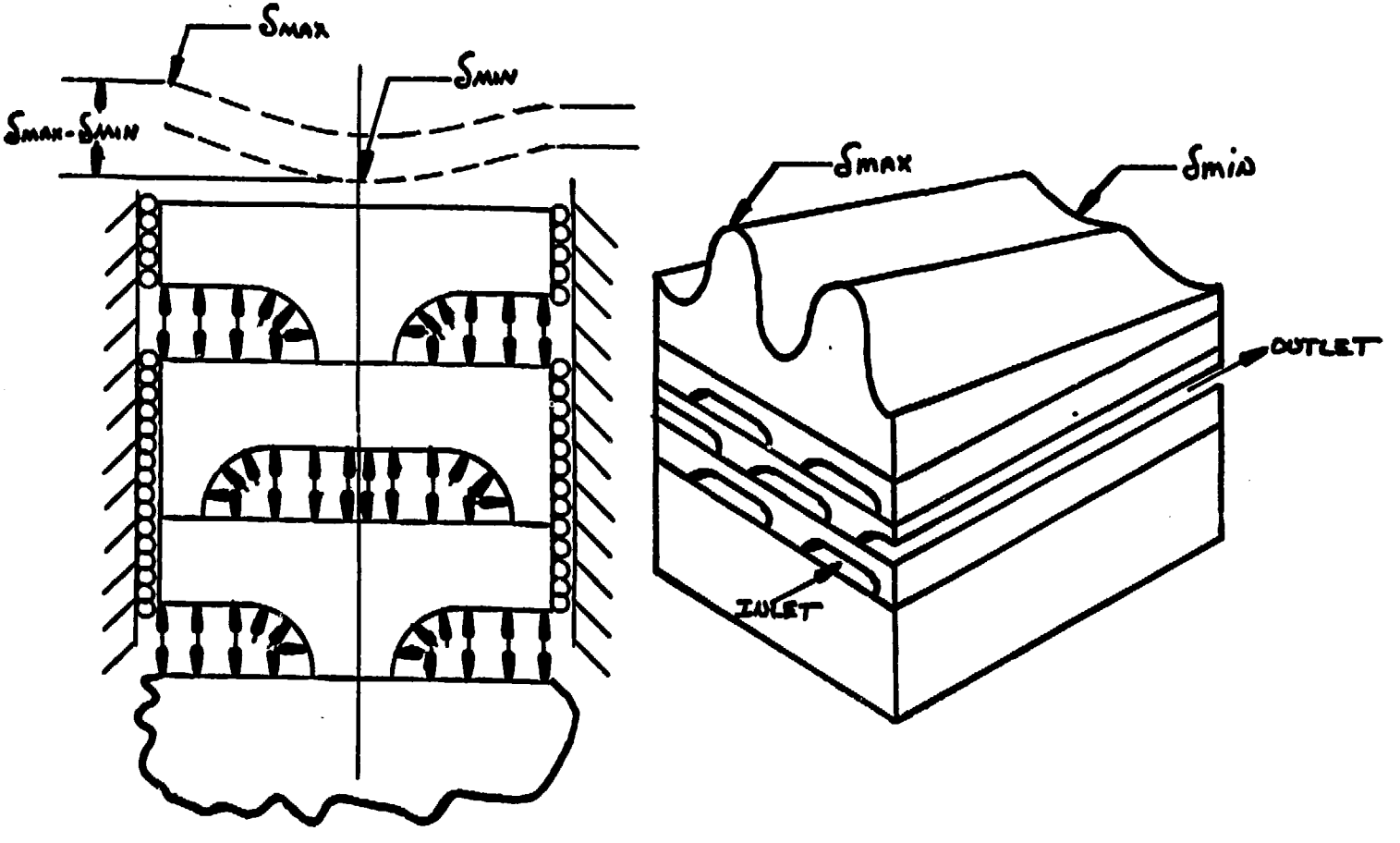

Figure 3. Classical Example of Pressure Tilt and Ripple

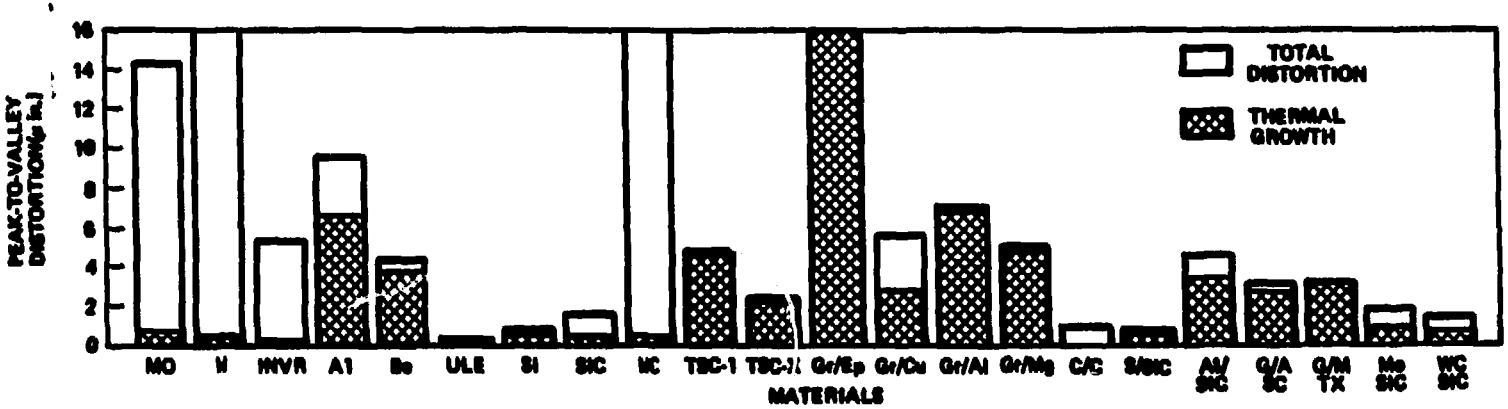

Figure 4. Comparison of resultant distortions for various mirror materials. HEX thickness varied to give constant weight design.

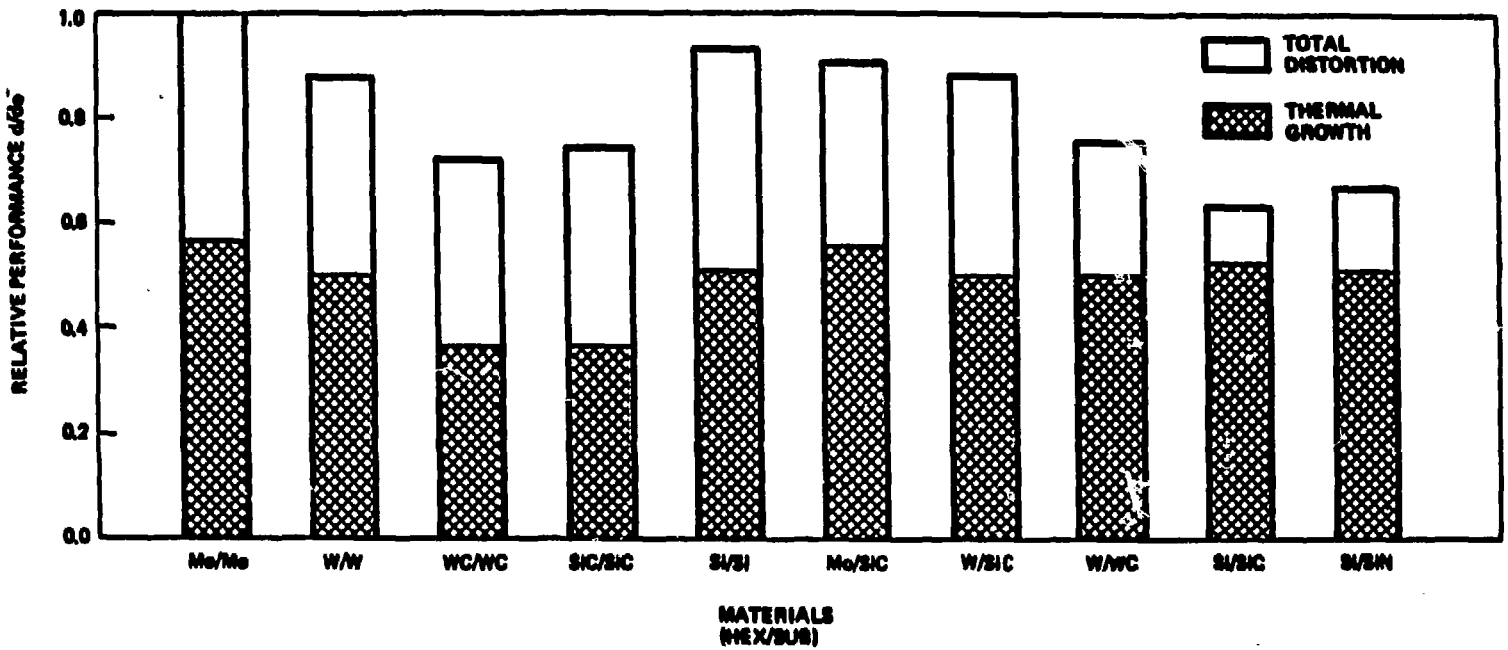

Figure 5. Mirror materials relative performance comparison for constant geometry and constant flow conditions. Molybdenum is the baseline material.

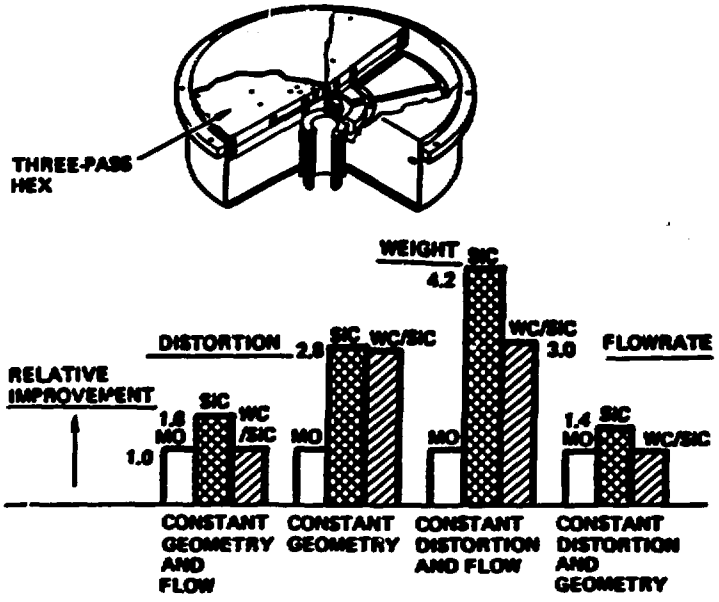

Figure 6. Parametric Analysis Results For Three-Pass Mirror Heat Exchanger

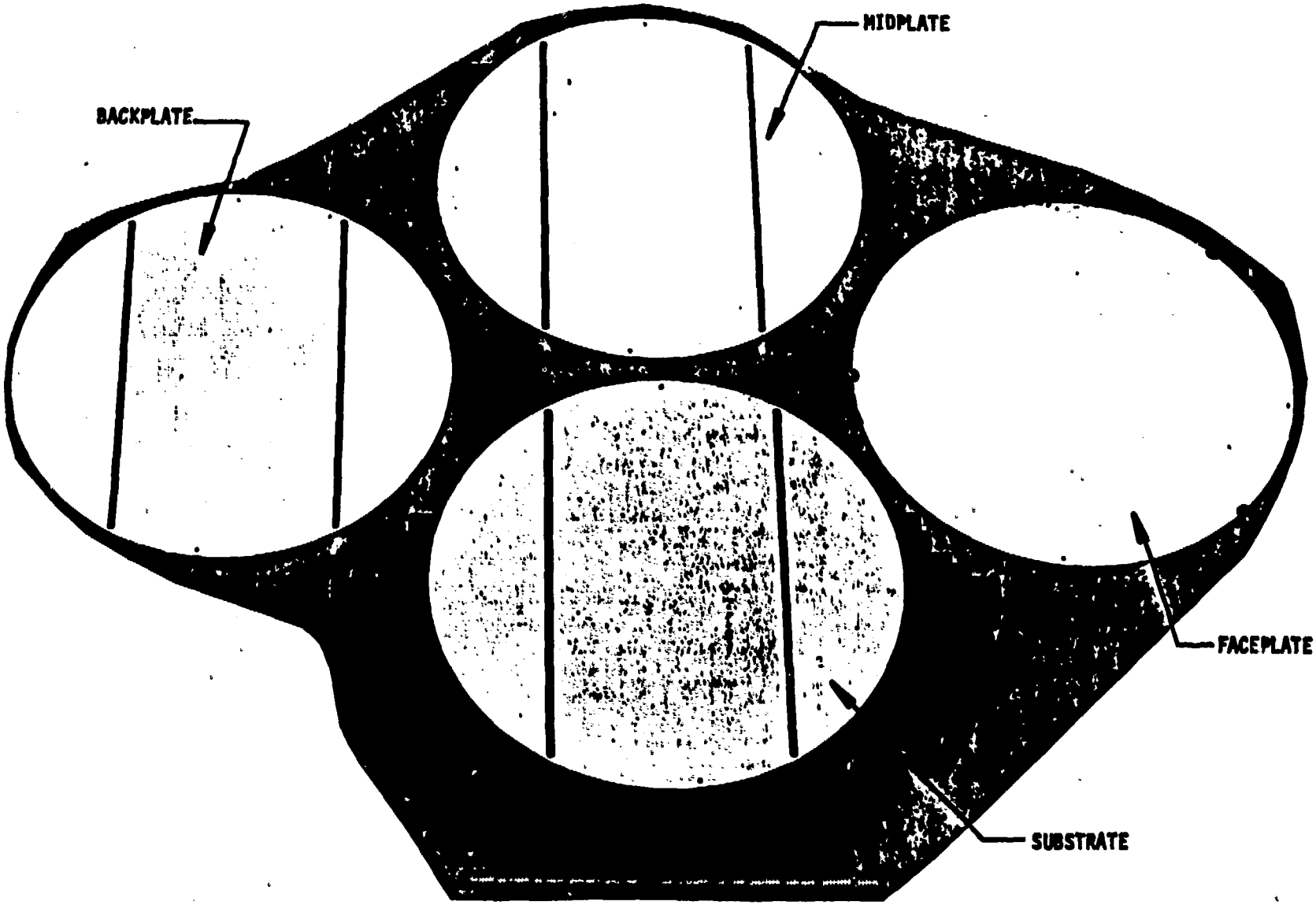

Figure 7. Typical Triple Pass Heat Exchanger Subassembly

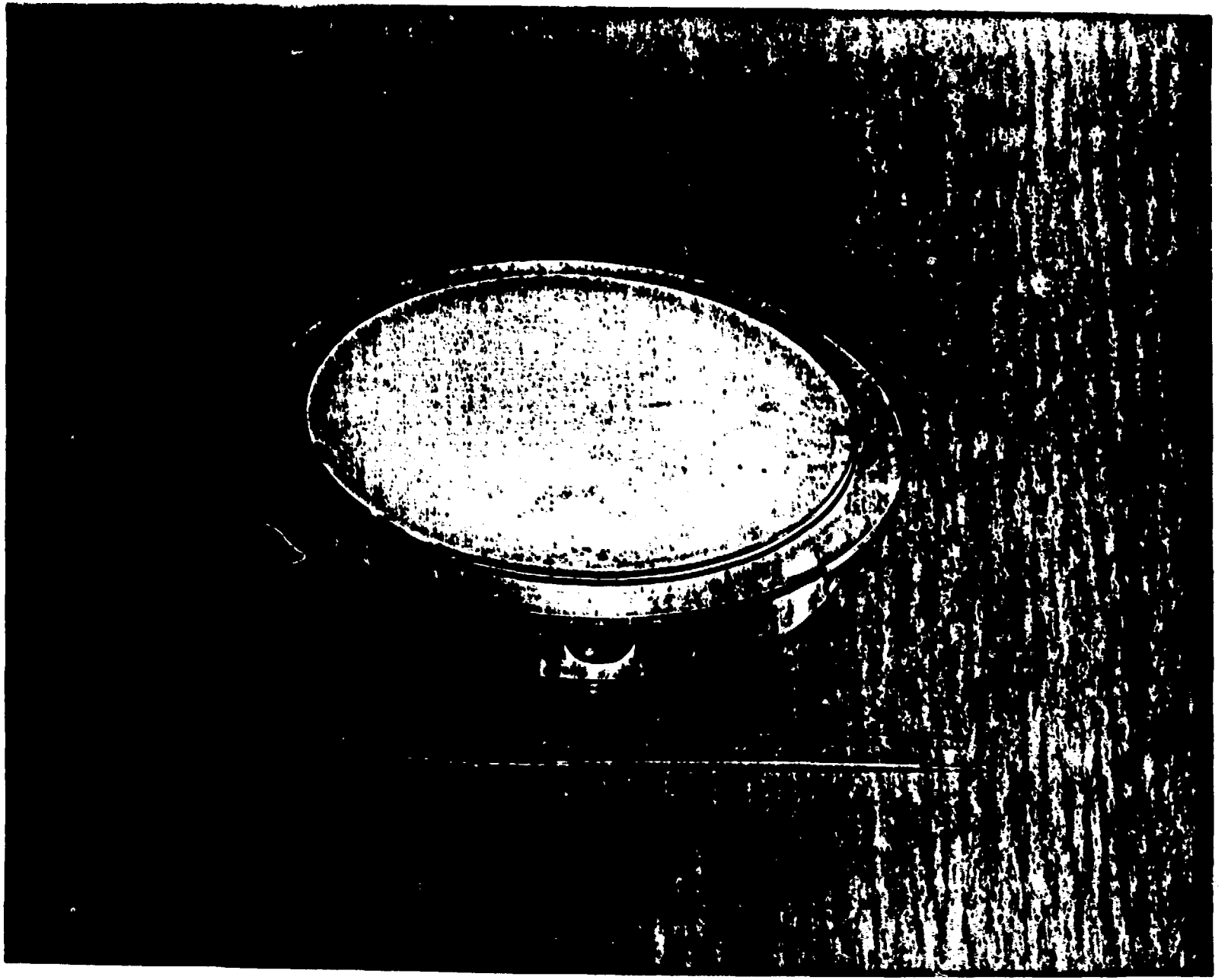

Figure 8. Typical Fabricated Heat Exchanger

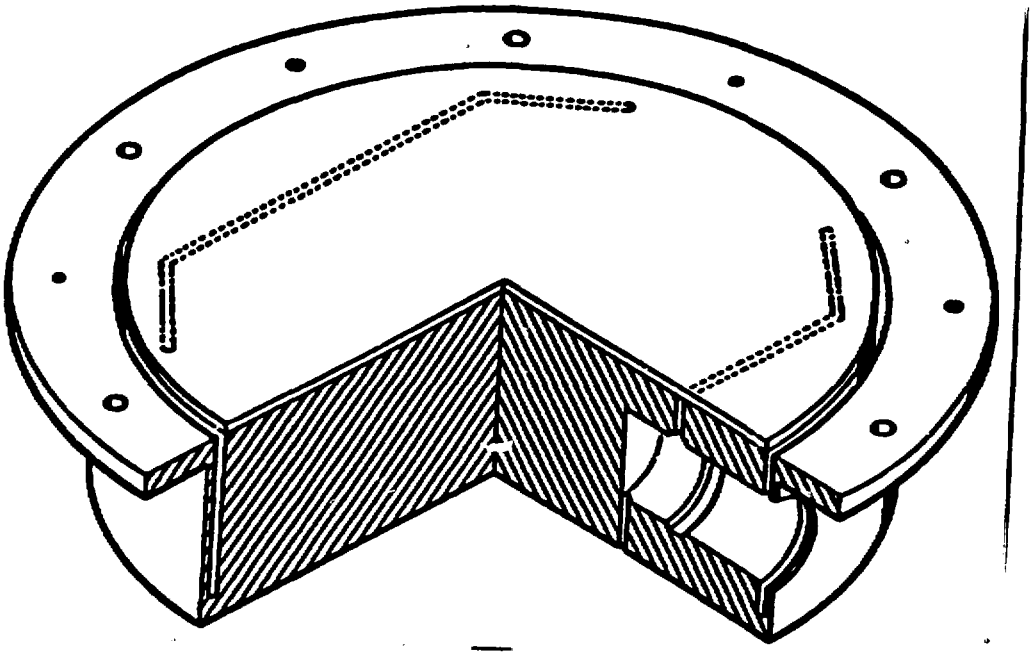

Figure 9. Typical Turning Flat Mirror Heat Exchanger Assembly

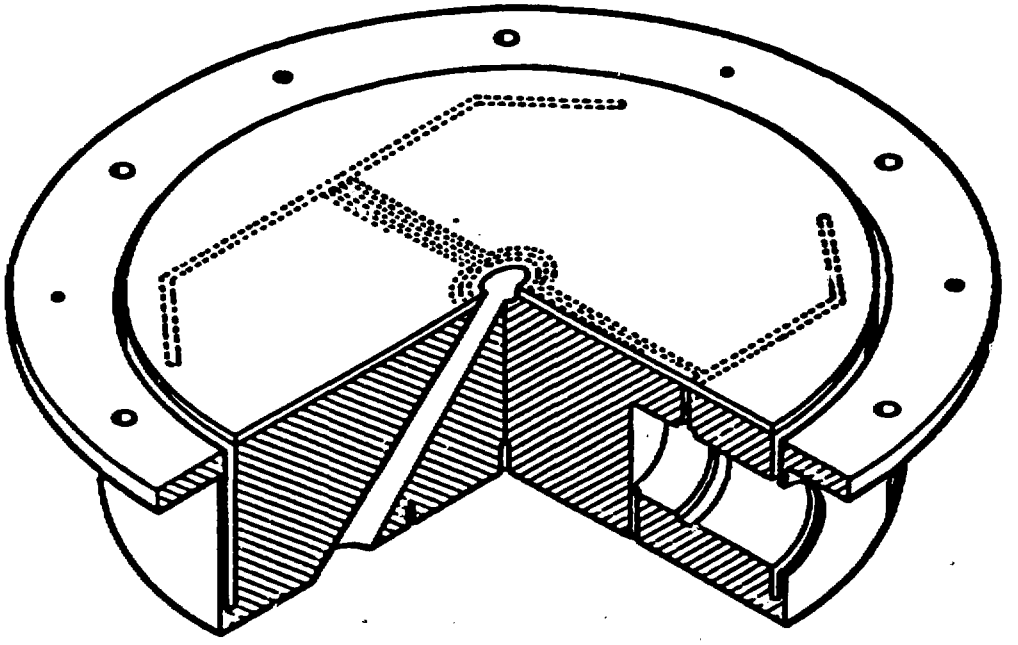

Figure 10. Typical Scraper Mirror Heat Exchanger Assembly

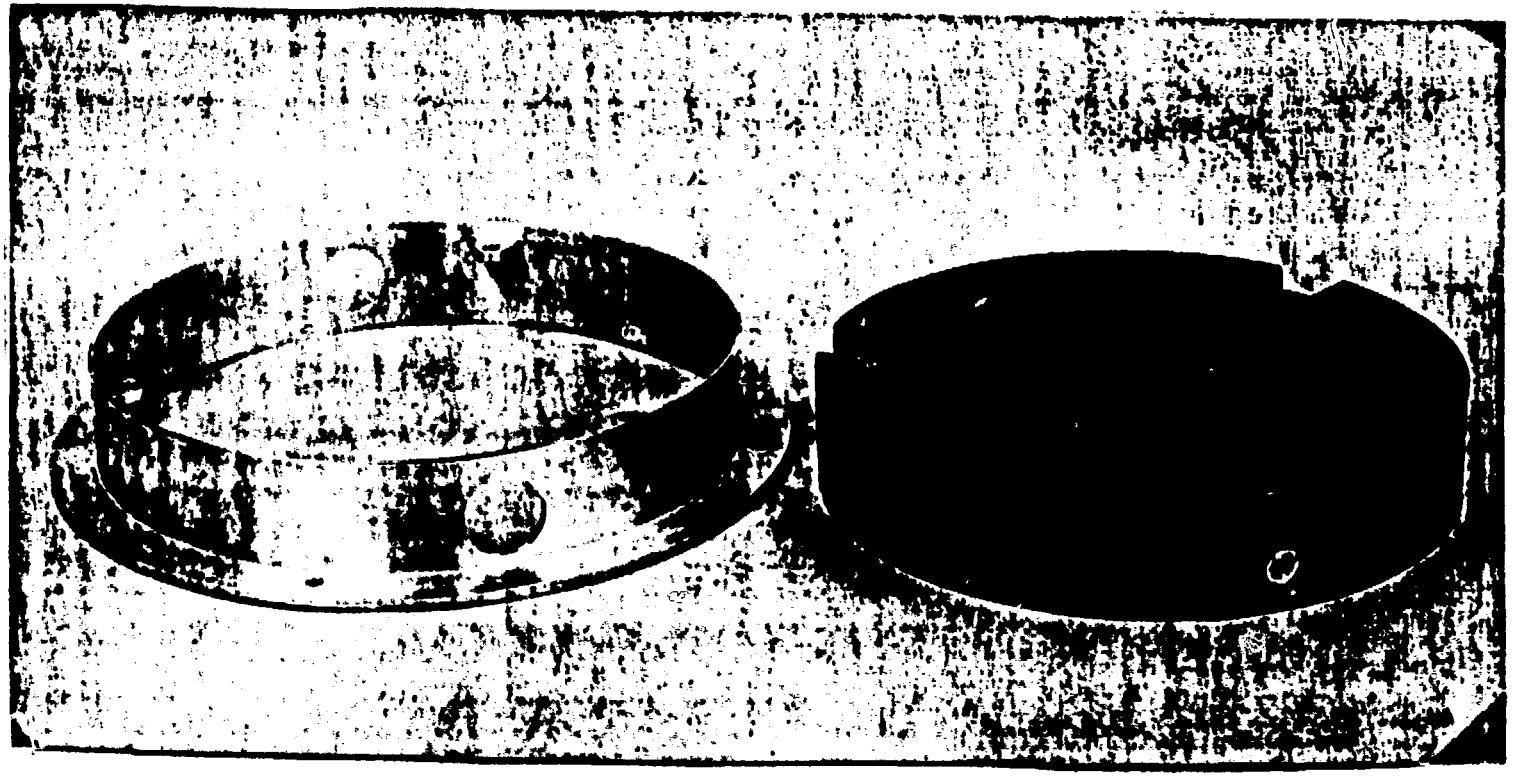

Figure 11. SiC Substrate and Steel Mount Ring

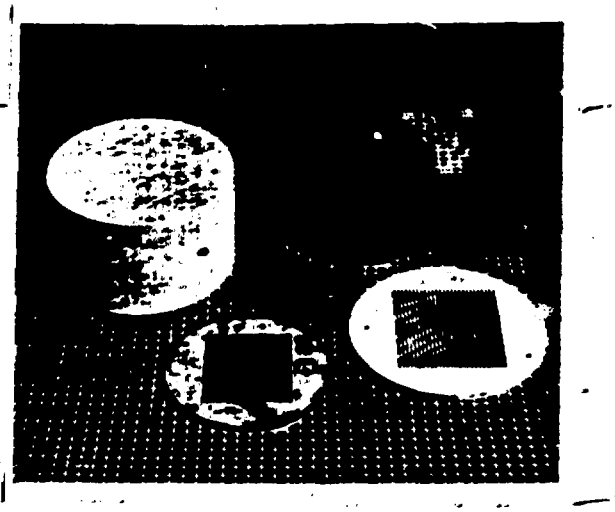

Figure 12. Green and Fully Sintered Alpha Silicon Carbide Mirror Heat Exchanger Assembly Details

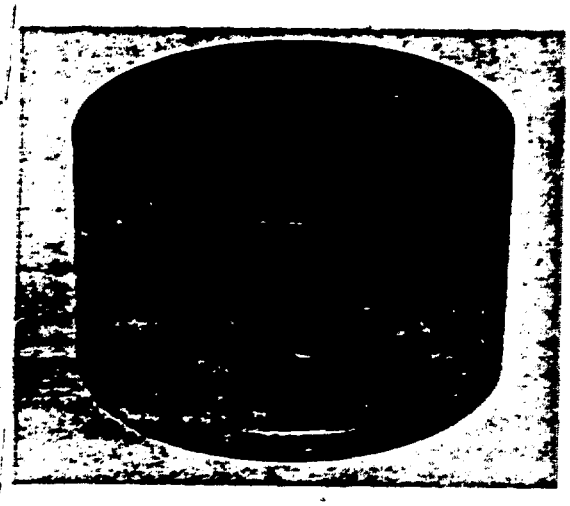

Figure 13. Diffusion Bonded Single-Pass Silicon Carbide Heat Exchanger

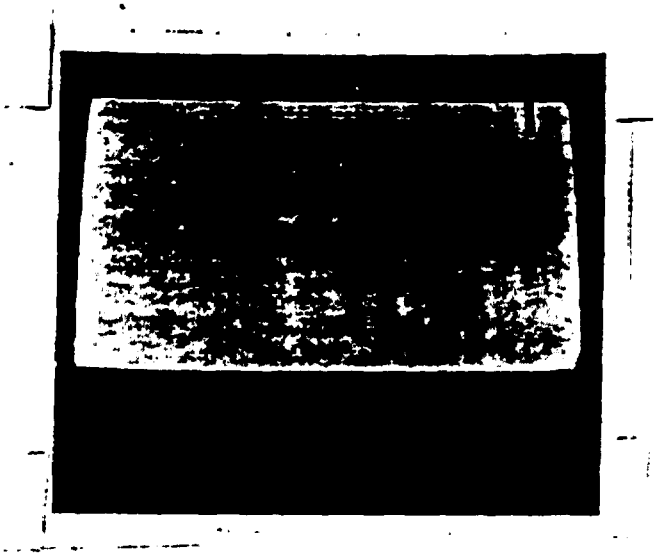

Figure 14. Cross-Sectioned Diffusion Bonded Silicon Carbide Heat Exchanger

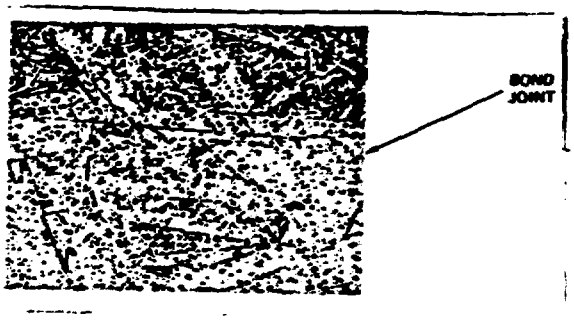

Figure 15. Photomicrograph (200X at the Diffusion Bond Joint)

ONE DIMENSIONAL MODEL

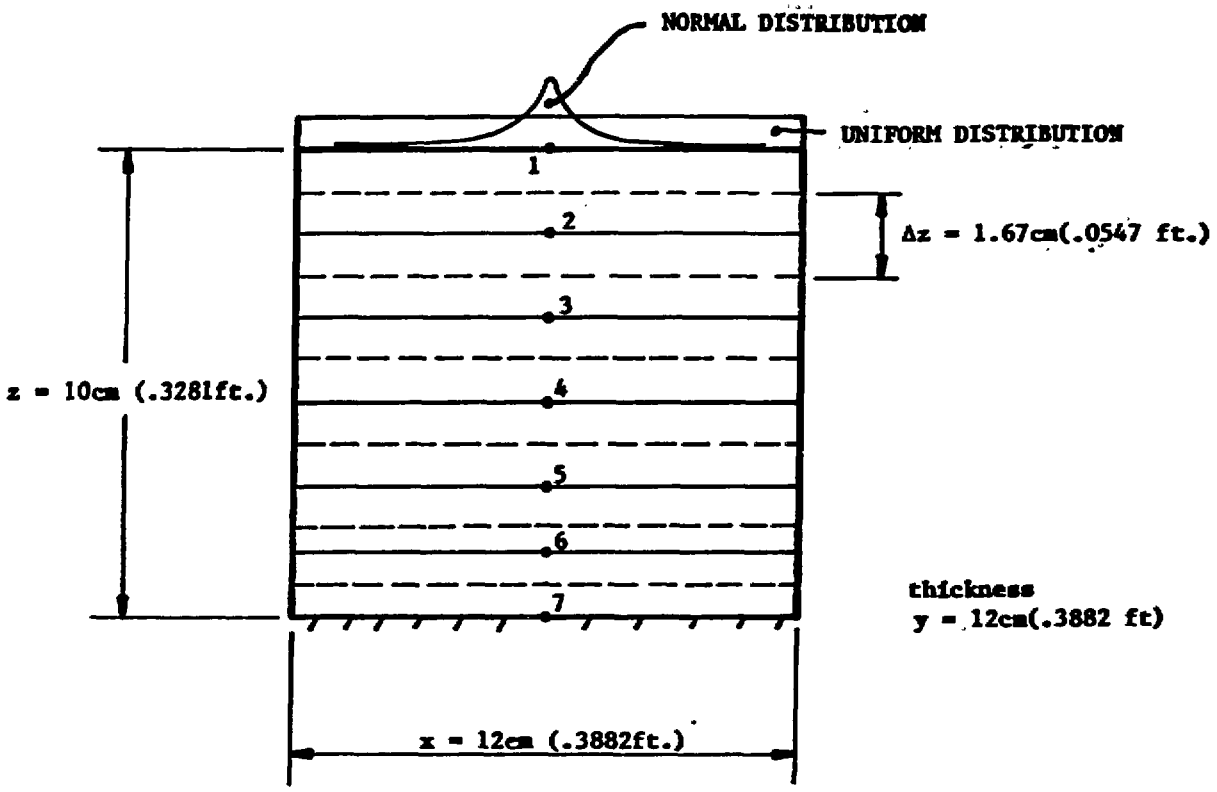

Figure 16. UNCOOLED DISCRETE THERMAL MODEL OF WIGGLER MIRROR

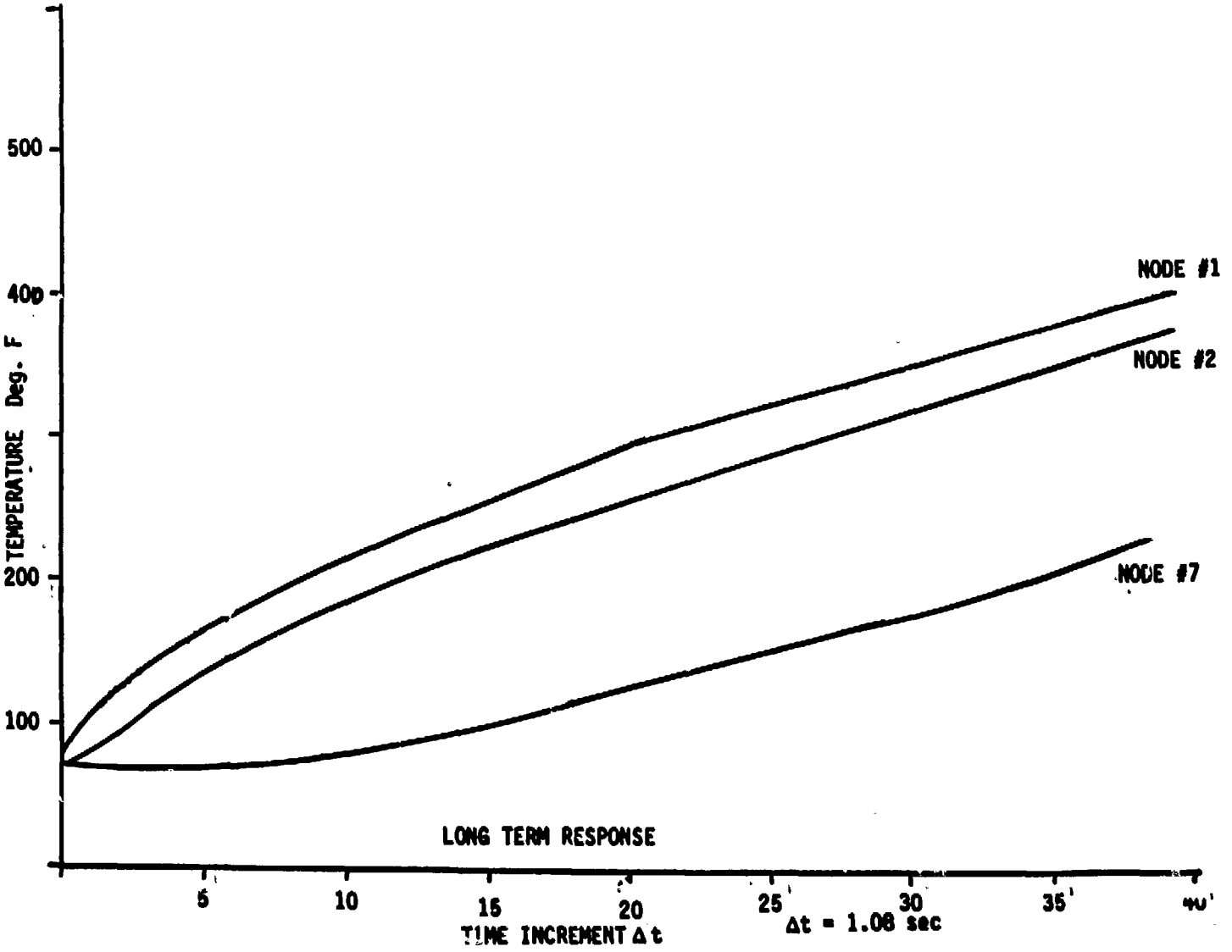

Figure 17. Thermal response of uncooled wiggler mirror at selected nodal analysis points.

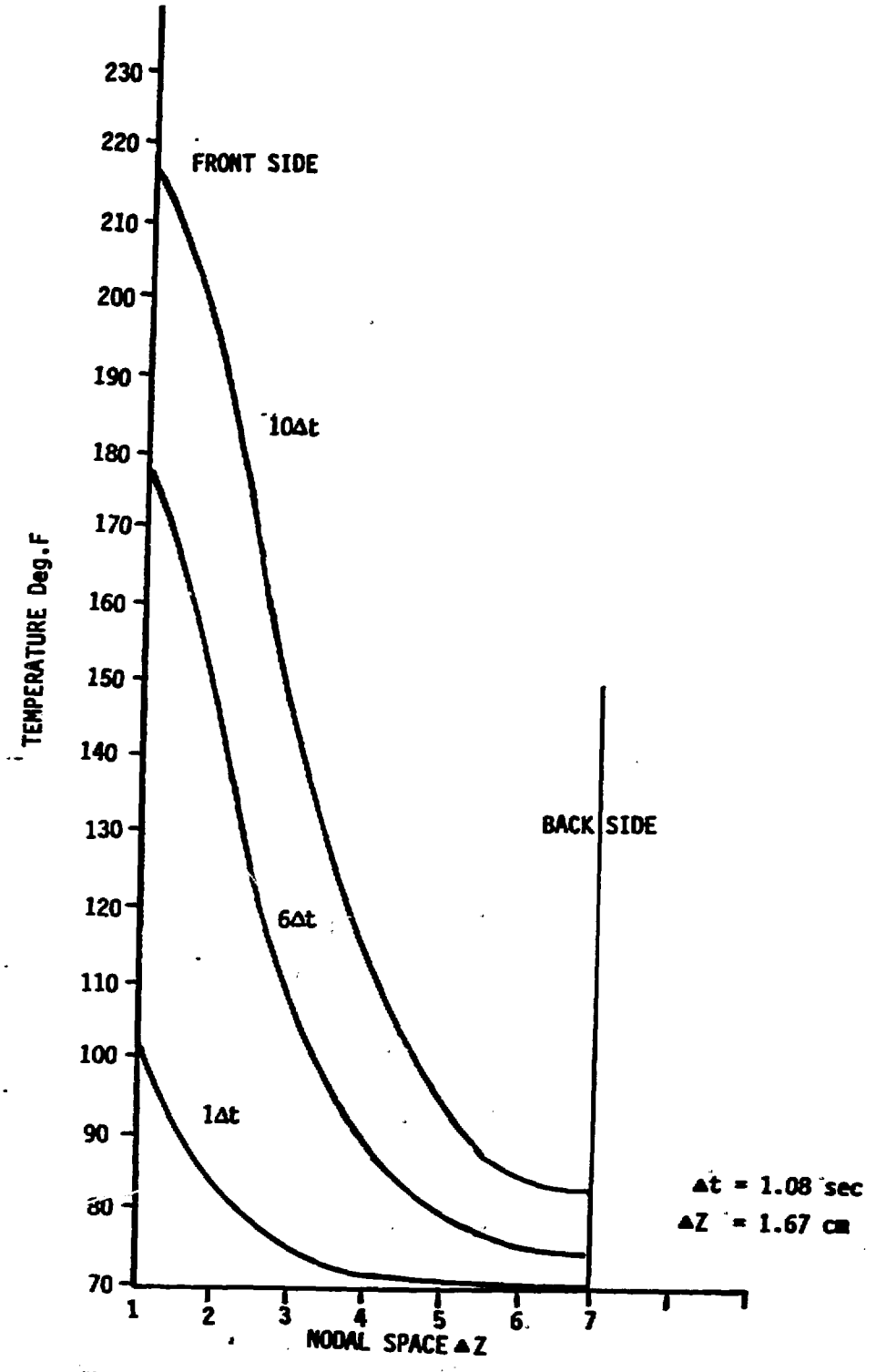

Figure 18. TEMPERATURE DISTRIBUTION OF UNCOOLED WIGGLER MIRROR